THE JOURNAL OF BIOLOGICAL CHEMISTRY
Vol. 276, No. 26, Issue of June 29, pp. 24232–24241, 2001
© 2001 by The American Society for Biochemistry and Molecular Biology, Inc.
Printed in U.S.A.

Dysbindin, a Novel Coiled-coil-containing Protein That Interacts with the Dystrobrevins in Muscle and Brain*

Received for publication, November 16, 2000, and in revised form, March 23, 2001
Published, JBC Papers in Press, April 20, 2001, DOI 10.1074/jbc.M010418200

Matthew A. Benson‡, Sarah E. Newey‡§, Enca Martin-Rendon¶‖, Richard Hawkes, and Derek J. Blake‡ ‡‡**

*From the ‡Department of Human Anatomy and Genetics, University of Oxford, South Parks Road, Oxford OX1 3QX, United Kingdom, the ¶Department of Biochemistry, University of Oxford, South Parks Road, Oxford OX1 3QU, United Kingdom, and the **Department of Cell Biology and Anatomy and Genes and Development Research Group, Faculty of Medicine, University of Calgary Faculty of Medicine, University of Calgary, Calgary, Alberta T2N 4N1, Canada*

The dystrophin-associated protein complex (DPC) is required for the maintenance of muscle integrity during the mechanical stresses of contraction and relaxation. In addition to providing a membrane scaffold, members of the DPC such as the α-dystrobrevin protein family are thought to play an important role in intracellular signal transduction. To gain additional insights into the function of the DPC, we performed a yeast two-hybrid screen for dystrobrevin-interacting proteins. Here we describe the identification of a dysbindin, a novel dystrobrevin-binding protein. Dysbindin is an evolutionary conserved 40-kDa coiled-coil-containing protein that binds to α- and β-dystrobrevin in muscle and brain. Dystrophin and α-dystrobrevin are co-immunoprecipitated with dysbindin, indicating that dysbindin is DPC-associated in muscle. Dysbindin co-localizes with α-dystrobrevin at the sarcolemma and is up-regulated in dystrophin-deficient muscle. In the brain, dysbindin is found primarily in axon bundles and especially in certain axon terminals, notably mossy fiber synaptic terminals in the cerebellum and hippocampus. These findings have implications for the molecular pathology of Duchenne muscular dystrophy and may provide an alternative route for anchoring dystrobrevin and the DPC to the muscle membrane.

Duchenne muscular dystrophy (DMD)[1] is the most common inherited muscle disease and is often associated with cognitive impairment. The DMD gene encodes dystrophin, a large membrane-associated protein that is expressed at highest levels in skeletal and cardiac muscle and in brain (1). Dystrophin is a component of the dystrophin-associated protein complex (DPC), a membrane-spanning oligomeric complex whose assembly is a prerequisite for normal muscle function (2–4). The loss of the DPC from the sarcolemma reduces the mechanical stability of the membrane compromising muscle function and eventually leading to muscle degeneration (5–7). In addition to their mechanical roles, dystrophin and the DPC are also involved in intracellular signaling, transducing extracellular cues to the cytoskeleton. This process is thought to play in important role in the molecular pathology of muscular dystrophy (8).

Recent experimental evidence has shown that α-dystrobrevin, a component of the DPC, may be involved in intracellular signaling (9). α-Dystrobrevin-deficient mice develop mild muscular dystrophy without disturbing the assembly of the DPC at the sarcolemma and altering the structural integrity of the muscle fiber (9). These mice have reduced levels of intracellular cGMP and have less neuronal nitric-oxide synthase (nNOS) at the sarcolemma (9). The role of nNOS in the pathology of muscular dystrophy is unclear since similar alterations in nNOS have been described in α-syntrophin-deficient mice; however, these mice do not develop muscular dystrophy (10).

The dystrobrevins are a family of dystrophin-related proteins that form, together with the syntrophins, the cytoplasmic component of the DPC. Two genes encode the dystrobrevins (11–15). α-Dystrobrevin is expressed at high levels in cardiac and skeletal muscle and the brain. Three major α-dystrobrevin isoforms, α-dystrobrevin-1, -2, and -3, representing successive C-terminal truncations are expressed in muscle (13, 16). α-Dystrobrevin-1 and -2 form complexes with dystrophin and the dystrophin-related protein utrophin in muscle. α-dystrobrevin-1 is concentrated at the NMJ, whereas α-dystrobrevin-2 is strongly expressed at the sarcolemma (16, 17). The second gene β-dystrobrevin is not expressed in adult muscle, but forms DPC-like complexes with dystrophin and the dystrophin isoform Dp71 in neurons (18). β-Dystrobrevin is enriched in the neuronal postsynaptic density along with dystrophin and is also found in axons and neuronal nuclei (18). The dystrobrevins are therefore a widely expressed family of binding partners for dystrophin, its isoforms, and the dystrophin-related protein utrophin.

The dystrobrevins bind to the C terminus of dystrophin through a reciprocal coiled-coil interaction involving the first putative helix of both proteins (19, 20). Dystrobrevin and dystrophin also bind directly to the syntrophin family of PDZ-containing proteins. This interaction is mediated by a short motif that is found in all dystrophin-related proteins and is adjacent to the first coiled-coil region (21). The PDZ domains of the syntrophin protein family bind to a variety of membrane-associated proteins, such as nNOS (22), MAST205 (23), stress-activated

* This work was supported in part by grants from the Wellcome Trust (to D. J. B.) and the Medical Research Council of Canada (to R. H.). The costs of publication of this article were defrayed in part by the payment of page charges. This article must therefore be hereby marked "*advertisement*" in accordance with 18 U.S.C. Section 1734 solely to indicate this fact.

The nucleotide sequence(s) reported in this paper has been submitted to the GenBank™/EBI Data Bank with accession number(s) AJ404859.

§ Recipient of a Wellcome Trust Prize studentship.

‖ Present address: Oxford BioMedica, Medawar Center, Oxford, OX4 4GA, United Kingdom.

‡‡ Wellcome Trust Senior Fellow. To whom all correspondence should be addressed. Tel./Fax: 44-1865-272183; E-mail: dblake@enterprise.molbiol.ox.ac.uk.

[1] The abbreviations used are: DMD, Duchenne muscular dystrophy; DPC, dystrophin-associated protein complex; GI, GenBank identifier; NMJ, neuromuscular junction; nNOS, neuronal nitric oxide synthase; kb, kilobase pair(s); PIPES, 1,4-piperazinediethanesulfonic acid; PCR, polymerase chain reaction; TBS, Tris-buffered saline; PBS, phosphate-buffered saline; RIPA, radioimmune precipitation assay.

This paper is available on line at http://www.jbc.org

Downloaded from http://www.jbc.org/ by guest on November 4, 2016

protein kinase-3 (24), and a class of sodium channels (25).

To determine the functional role of the dystrobrevins in muscle and brain, we have performed a yeast two-hybrid screen to identify dystrobrevin-binding partners. In this paper, we describe the cloning and characterization of dysbindin, a 40-kDa coiled-coil-containing protein that binds to both α- and β-dystrobrevin in muscle and brain.

EXPERIMENTAL PROCEDURES

Yeast Two-hybrid Screening—The entire β-dystrobrevin coding region was amplified by PCR and cloned into the *Eco*RI/*Sal*I sites of the bait plasmid pHybLex/Zeo (Invitrogen). Transforming this plasmid into *S. cerevisae* L40 created a bait strain that was then co-transformed with an adult mouse brain cDNA library in pJG4–5 (Origene) or a mouse $H2K^b$-tsA58 myotube cDNA library in pYESTrp2 (26) as described elsewhere (27). Potential interacting clones were identified by plating the transformation on minimal media lacking histidine, tryptophan, lysine, and uracil containing 5 mM 3-aminotriazole and 300 μg/ml Zeocin. Yeast clones that grew on histidine-deficient media were assayed for β-galactosidase activity as per manufacturer's instructions (Invitrogen). The α-syntrophin prey (amino acids 272–503) was made by cloning the *Sac*I/*Eco*RI fragment from a mouse α-syntrophin cDNA clone into pYesTrp2. The Fos and Jun bait and prey control plasmids were supplied by the manufacturer (Invitrogen). Prey plasmids were isolated from yeast and transformed by electroporation into *Escherichia coli* XL1-Blue using standard methods. The 5′ and 3′ ends of each clone were sequenced using vector primers.

Sequence Analysis and Expression—The dysbindin cDNA sequence (EMBL accession no. AJ404859) was obtained by sequencing the largest cDNA clone (m10) identified in the screen (Fig. 1*B*). Protein sequence alignments were made using the program PSI-BLAST (28), and coiled-coils were predicted using the program COILS (29) using a window of 28 residues and no weighting. Mouse multiple tissue Northern blots were purchased from Origene and were hybridized with the m10 cDNA or a β-actin cDNA in Rapid-hyb buffer (Amersham Pharmacia Biotech). The hybridized blots were processed as described previously (30).

Protein extracts were prepared for Western blotting by homogenizing fresh tissue or cells in SDS/urea buffer (4 M urea, 3.8% SDS, 20% glycerol, 75 mM Tris, pH 6.8, 5% 2-mercaptoethanol). 40 μg of protein were separated on 10% SDS-polyacrylamide gels and transferred to nitrocellulose membranes as described previously (15). Proteins were detected with the appropriate antibody using a BM chemiluminescence detection kit (Roche Molecular Biochemicals). Blot densitometry was performed on radiographic film using an Alpha Imager and software (Alpha Innotech Corp.).

Antibodies—The region encoding amino acids 196–352 was amplified by PCR, cloned into pET32(a) (Novagen), and transformed into *E. coli* BL21(DE3) Gold (Stratagene). The fusion protein was purified using Talon resin (CLONTECH) as per manufacturer's instructions. The fusion partner was removed by thrombin digestion and affinity chromatography. The remaining protein was used to immunize New Zealand White rabbits using standard protocols. All antisera were immunoaffinity-purified as described previously (18). Antibody specificity was determined by pre-absorption of the m10CT-FP antisera diluted 1:25 in Tris-buffered saline (TBS; 150 mM NaCl, 50 mM Tris, pH 7.5) with 100 μg/ml (2 μM) of the immunizing fusion protein for 1 h at room temperature. The pre-absorbed serum was used as described below.

The dystrobrevin antibodies, β521 (which only detects β-dystrobrevin) and βCT-FP (which detects β-dystrobrevin and α-dystrobrevin-1 and -2), the anti-dystrophin antibody 2166, and the anti-utrophin antibody URD40 have been described elsewhere (15, 18). The 9E10 monoclonal anti-Myc antibody was purchased from Covance. The anti-dystrobrevin monoclonal antibody, clone 23, was purchased from Transduction Laboratories. The anti-syntrophin monoclonal antibody SYN1351 was kindly provided by Prof. Stanley C. Froehner (31). The MANDRA1 anti-dystrophin monoclonal antibody was kindly supplied by Prof. Glenn Morris (32).

Expression Constructs—The mammalian expression constructs used in this study are listed in Table I. m10:pCIneo was made by cloning the entire dysbindin cDNA into the *Eco*RI/*Sal*I sites of pCIneo. A c-Myc epitope tag was introduced into the N terminus dysbindin by PCR with the following primers; m10myc (5′-TGAATCATGGAGCAAAAGCTCATTTCTGAAGAGGACTTGCTGGAGACCCTGCGCGA) and m10–1310R (5′-ATCTCGAGCCATAAGCTTTATTGTGAGC). The 1.2-kb PCR product was subcloned into pCIneo to produce myc-m10:pCIneo. The BetaG expression construct and derivatives thereof (Table I) were made from a full-length β-dystrobrevin cDNA clone. BetaG was made by subcloning the entire β-dystrobrevin cDNA into the *Not*I site of pCIneo. The same insert was subcloned into the *Not*I site of pGEM-13Zf(+) to produce a recombinant intermediate plasmid (BetaG:pGEM13) that was used to make the following deletion constructs. BetaGΔH1 was made by digesting BetaG:pGEM13 with *Nhe*I, removing the 201-base pair stuffer fragment and re-circularizing. The insert from this plasmid was cloned into pCIneo. BetaGΔH1+2 was produced by digesting BetaG:pGEM13 with *Nhe*I and *Bst*EII. The stuffer was removed and replaced with the annealed primers CC2F (5′-CTAGCGCTAAAGGAGGAAGAGCAAAAGCAGGCAGCTCAAGCCACAGG) and CC2R (5′-GTGACCCTGTGGCTTGAGCTGCCTGCTTTTGCTCTTCCTCCTTTAGCG). This sequence replaces the alternatively spliced "b-site" of β-dystrobrevin that is immediately adjacent to the second coiled-coil (15). The insert was excised and subcloned into pCIneo. BetaGΔH2 was made by ligating the 201-base pair *Nhe*I fragment into the *Nhe*I site of BetaGΔH1+2. The α-dystrobrevin-1 expression construct m24:pCIneo was made by subcloning the 2.8-kb *Not*I/*Spe*I restriction fragment from m24 (12) into pCIneo. pG-utro was constructed by digesting clone au#3 (33) with *Xba*I and *Ase*I, end-filling with Klenow DNA polymerase, and subcloning into pcDNA3 (Invitrogen). pDp116 was constructed by cloning the 3.5-kb *Eco*RI fragment from clone 22D (34) into pcDNA3. The β_2-syntrophin construct was made by subcloning the 2.8-kb *Eco*RI/*Xho*I insert from a mouse β_2-syntrophin partial cDNA clone in pBluescript (kindly provided by Prof. Stanley Froehner) (35) into pCIneo.

Transfection—COS-7 cells were grown on glass coverslips and transfected with between 0.5 and 2 μg/3.5-cm^2 well of plasmid DNA using Fugene-6 (Roche). After 24 h, the transfected cells were washed thoroughly in PBS, fixed in ice-cold 4% paraformaldehyde, and permeabilized with 0.1% Triton X-100. The cells were washed thoroughly in PBS and blocked in 10% normal donkey serum. Primary antibodies were applied for 1 h at room temperature in PBS. After washing, the coverslips were incubated with the secondary antibody for an additional 1 h. After several washes, the coverslips were mounted in Vectashield (Vector Laboratories) and viewed under a Leica TCS confocal microscope. Images were captured using Leica TCS Powerscan software.

Immunocytochemistry—Immunocytochemistry on frozen muscle sections was carried out as described previously (16). Sections were labeled with m10CT-FP at a dilution of 1:50 or βCT-FP at a dilution of 1:200 in TBS. Neuromuscular junctions were identified with Alexa 488-conjugated α-bungarotoxin (Molecular Probes). Double immunofluorescence on muscle sections was performed using 10-fold excess of Rhodamine Red-X-labeled donkey anti-rabbit $F(ab')_2$ fragments as described by the supplier (Jackson Immunoresearch). After extensive washing in TBS, the second antibody was applied as described above. Sections were examined by fluorescence microscopy using a Leica DMRE microscope or by confocal microscopy using a Leica TCS microscope.

For brain immunocytochemistry, tissue was processed as described previously (18). Sections were cut at 10–20 μm in the transverse or sagittal planes, mounted on gelatin-coated slides, and stained with m10CT-FP at a dilution of 1:200. Indirect peroxidase immunocytochemistry was performed on the slide as described previously (36). Photomicrographs were captured with a SPOT Cooled Color digital camera (Diagnostic Instruments Inc.) and assembled in Adobe Photoshop 4.0. The images were cropped and corrected for brightness and contrast but not otherwise manipulated.

Immunoprecipitation—Fresh rat muscle and brain (2 g) were homogenized in CSK buffer (300 mM sucrose, 100 mM NaCl, 10 mM PIPES, pH 6.8, 3 mM $MgCl_2$, 1 mM EGTA, 0.5% Triton X-100, plus protease inhibitors (Sigma)). After incubation on ice for 30 min, the homogenates were clarified by centrifugation at 141,000 × *g*. Proteins were immunoprecipitated with 4 μg of m10CT-FP or 4 μg of the anti-dystrobrevin monoclonal antibody as described previously (18). Immune complexes were washed extensively in CSK buffer, eluted in SDS/urea buffer, and analyzed by Western blotting.

For immunoprecipitation of heterologously expressed proteins, 2×10^6 COS-7 cells were co-transfected with 10 μg of myc-m10:pCIneo and 2 μg of the β-dystrobrevin-encoding plasmids (Table I) or 10 μg of m24:pCIneo using Fugene-6. After 24 h the cells were washed in PBS and lysed with 5 ml of RIPA buffer (150 mM NaCl, 50 mM Tris pH 8.0, 1% Triton X-100, 1% sodium deoxycholate, 0.1% SDS, 2.5 mM EDTA, plus protease inhibitors). Cell extracts were clarified by centrifugation at 50,000 × *g* for 30 min. Proteins were immunoprecipitated with either 4 μg of m10CT-FP or 4 μg of 9E10 as described above. Immunoprecipitated proteins were eluted in SDS/urea buffer and analyzed by Western blotting.

Downloaded from http://www.jbc.org/ by guest on November 4, 2016

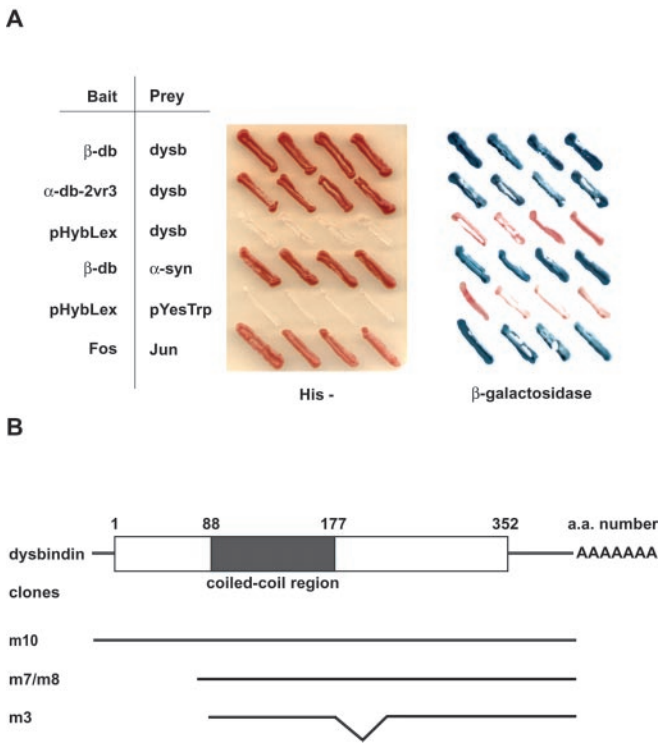

FIG. 1. **Two-hybrid analysis of the dysbindin:dystrobrevin interaction.** *A*, different combinations of bait and prey plasmids were co-transformed into yeast and assayed for growth on histidine-deficient media and β-galactosidase activity. Interacting clones grow on media lacking histidine (*His*−) and have high levels of β-galactosidase activity as indicated by the blue coloration on the filter lift. *β-db*, β-dystrobrevin; *α-db-2vr3*, α-dystrobrevin-2 containing the muscle-expressed vr (variable region) 3 sequence (12); *dysb*, dysbindin; *α-syn*, α-syntrophin. *B*, the distribution of the different interacting clones isolated from the mouse brain cDNA library. Clone m3 has a deletion of amino acids 171–222. Muscle-derived clones, although different, all started in the 5′-untranslated region of the dysbindin cDNA. The location of the predicted coiled-coil domain (see below) is indicated.

RESULTS

Yeast Two-hybrid Screening—In order to identify proteins that interact with the dystrobrevins in muscle and in the brain, yeast two-hybrid screens were performed with a bait plasmid containing the entire mouse β-dystrobrevin coding sequence. Approximately 6×10^5 and 2×10^6 independent transformants were screened from the mouse brain and H2K mouse myotube cDNA libraries, respectively. This screen resulted in the isolation of 10 clones from the brain library and 52 clones from the muscle library. End sequencing of these clones revealed that four and nine clones from each library were derived from the same gene. To reflect the binding capabilities of the protein encoded by these cDNA clones, we have named this protein dysbindin. Several dysbindin cDNAs were also identified in a yeast two-hybrid screen of the H2K library using α-dystrobrevin-2 as a bait. In addition, the two-hybrid screens identified all the known dystrobrevin-binding proteins, dystrophin, utrophin, and the syntrophins, confirming the efficacy of the technique. Interestingly, no clones encoding signaling proteins such as kinases and guanine nucleotide exchange factors were identified in any of the screens. The specificity of the protein:protein interactions in yeast was confirmed by co-transforming different bait and prey plasmids (Fig. 1*A*). Dysbindin interacts with both and β- and α-dystrobrevin-2 but does not transactivate reporter gene expression when co-transformed with the empty bait plasmid pYesTrp2. In control experiments, β-dystrobrevin also interacted with the C terminus of α-syntrophin an interaction that is known to occur physiologically (37, 38). The transcription factors Fos and Jun were used as additional positive control for interacting proteins while the empty bait and prey vectors failed to transactivate reporter gene expression when co-transformed (Fig. 1*A*).

Cloning and Characterization of Dysbindin—The yeast two-hybrid system identified several similar clones that were sequenced (Fig. 1*B*). The largest clone m10 was 1.4 kb and had a poly(A) tail at the 3′ end. The complete sequence of the m10 cDNA and the deduced amino acid sequence is shown in Fig. 2*A*. The m10 cDNA encodes dysbindin, a protein of 352 amino acids with a predicted molecular mass of 39.7 kDa and a pI of 4.6. To determine whether dysbindin was part of previously characterized protein family and to identify any known domains, an unfiltered PSI-BLAST data base search (28) was initiated. Two proteins in the data base were found to be significantly similar to dysbindin. These are the human hypothetical protein CAB83042 (E-value, 3e-20) and the *Drosophila* predicted protein CG6856 (E-value, 2e-19). The sequence similarity between dysbindin and these proteins is depicted in Fig. 2*B*. The percentage sequence identities between dysbindin and CAB3042 and CG6856 are 45.5% over 135 amino acids and 31.5% over 211 amino acids, respectively. CAB83042 encodes a dysbindin-related protein that has been described in several unpublished cDNA sequencing projects (GI 7689032, uncharacterized hypothalamus protein HSMNP1; GI 7340749, hypothetical protein STRAIT; GI 7020689, unnamed protein encoded by KAT10570). In addition to these proteins, dysbindin orthologues are present in *Danio rerio* and *Xenopus laevis*. No documented protein domains were identified in dysbindin however, computer-aided sequence analysis demonstrated that dysbindin contains a predicted coiled-coil region between amino acids 88 and 177 (Fig. 2*C*). This prediction is also true of the proposed *Drosophila* orthologue of dysbindin, CG6856 (Fig. 2*C*).

An alternatively spliced cDNA (m3) corresponding to a deletion of amino acids 171–222 was also identified in the two-hybrid screen. This clone interacts robustly with dystrobrevin (Fig. 1*B*). It is possible that the expression of this splice variant gives rise to the additional lower molecular weight band seen on Western blots (Fig. 3*B*).

To determine the expression pattern of the dysbindin transcript, a multiple tissue Northern blot was hybridized with the complete m10 cDNA clone. A 1.4-kb transcript was detected at varying levels in all of the tissues examined (Fig. 3*A*, *upper panel*). The highest levels of dysbindin expression were in testes, liver, kidney, brain, heart, and lung. The dysbindin mRNA is also expressed in skeletal muscle and in the stomach and small intestine, two tissues that contain significant amounts of smooth muscle. Hybridization of the same blot with a β-actin cDNA probe showed that each lane contains similar amounts of mRNA (Fig. 3*A*, *lower panel*).

To determine the tissue distribution of dysbindin, an antibody (m10CT-FP) was raised against the last 156 amino acids of the protein. The anti-dysbindin antibody was affinity-purified and used for Western blotting. A 50-kDa protein is detected at varying levels in all the tissues examined (Fig. 3*B*). Dysbindin is resolved as a protein doublet in the different tissues presumably reflecting alternative splicing within the gene (see above). The doublet is only resolved on shorter exposures or when longer electrophoresis times are used. The relative mobility of dysbindin expressed in COS-7 cells is identical to the protein detected with m10CT-FP detected in the tissue extracts (Fig. 3*B*). The high relative mobility of dysbindin is probably due to the content of acidic amino acids in the primary sequence.

In Vitro Association of Dysbindin with Dystrobrevin—To determine whether dysbindin binds directly to the dystrobrevins

Downloaded from http://www.jbc.org/ by guest on November 4, 2016

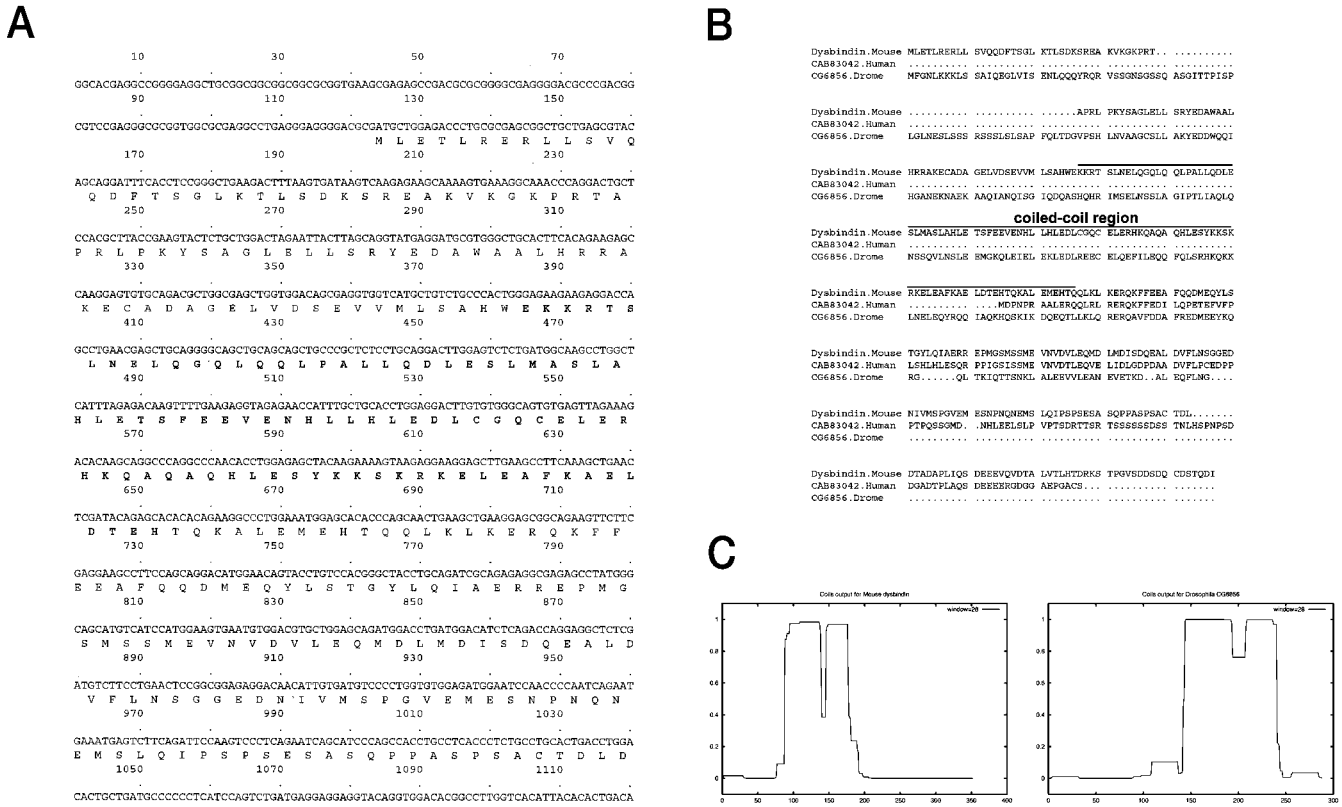

FIG. 2. **Sequence analysis.** *A*, sequence of mouse dysbindin. The complete cDNA sequence and conceptual translation are shown. The sequence in *bold lettering* corresponds to the predicted coiled-coil domain. The *underlined* sequence is the consensus site for polyadenylation. The predicted relative molecular mass of dysbindin is 39.7 kDa with a pI of 4.6. *B*, dysbindin homologues. The sequence alignment shows dysbindin aligned with the *Drosophila* protein, and the human hypothetical protein CAB83042. The human dysbindin homologue has significant sequence similarity to the C terminus of dysbindin but lacks the indicated predicted coiled-coil region. *C*, coiled-coil prediction. Dysbindin has a coiled-coil region that spans 89 amino acids (amino acids 88–177). The coiled-coil prediction is interrupted between residues 138 and 146, potentially yielding two distinct coil-coils as predicted for the dystrophin family of proteins (19). The *Drosophila* dysbindin orthologue, CG6856, has a similar coiled-coil region spanning 96 amino acids (144–240) with an interruption between amino acids 193 and 208.

and other members of the dystrophin protein family, COS-7 cells were transiently transfected with myc-m10:pCIneo in combination with other expression constructs encoding dystrophin-related proteins and mutants thereof (Table I). Prior to these studies, the cellular distribution of β-dystrobrevin and dysbindin was determined in cells transfected with only the cognate plasmids. β-Dystrobrevin is located in intensely staining punctae distributed throughout the cell (Fig. 4*A*). β-Dystrobrevin immunoreactivity was concentrated in punctae around the nucleus but rarely seen in the periphery of transfected cells. By contrast, dysbindin is expressed diffusely in the cytoplasm of transfected cells (Fig. 4*B*). Dysbindin immunoreactivity is also concentrated in the nucleus of transfected cells (Fig. 4, *B* and *C*). A c-Myc epitope tag was introduced into the N-terminal encoding region of the dysbindin cDNA for the purposes of co-localization. The N terminus of dysbindin was chosen for epitope tagging because our two-hybrid analysis indicated that the C terminus of dysbindin contained the dystrobrevin binding site (Fig. 1*B*). This construct is also localized to the cytoplasm of transfected cells, indicating that the epitope tag has no apparent effect on the cellular distribution of dysbindin (Fig. 4*C*). When the constructs encoding dysbindin (myc-m10:pCIneo) and β-dystrobrevin (BetaG) are co-transfected, dysbindin expression causes the dramatic re-localization of β-dystrobrevin into a diffuse cytoplasmic pattern (Fig. 4, *D–F*). It is interesting to note that, although dysbindin and β-dystrobrevin are co-localized in the cytoplasm, they do not co-localize in the nucleus (Fig. 4*F*). A similar pattern is also seen with syntrophin and β-dystrobrevin (Fig. 4*L*), suggesting that β-dystrobrevin is excluded from the nucleus.

Sequence analysis suggests that dysbindin and the dystrobrevins are coiled-coil-containing proteins. To determine whether the putative dystrobrevin coiled-coil domain is important for the interaction with dysbindin, we constructed three mutant β-dystrobrevin proteins that lack one or the other of the coiled-coils, or both (Table I). Each construct was designed so that it would remove the coiled-coil region while preserving the syntrophin-binding site (21). The mutated β-dystrobrevin proteins were all expressed at high levels and could be detected with the antibody β521. When these constructs were transfected into COS-7 cells, each gave the same punctate immunoreactivity as the wild type protein (data not shown). The ability of dysbindin to re-distribute β-dystrobrevin to the cytoplasm was determined by co-transfection of myc-m10:pCIneo with each of the mutants. In all cases, dysbindin expression successfully re-localized the mutant dystrobrevins to the cytoplasm (Fig. 4, *G–I*). These data suggest that both coiled-coils are not essential for the interaction of dysbindin with dystrobrevin and

Downloaded from http://www.jbc.org/ by guest on November 4, 2016

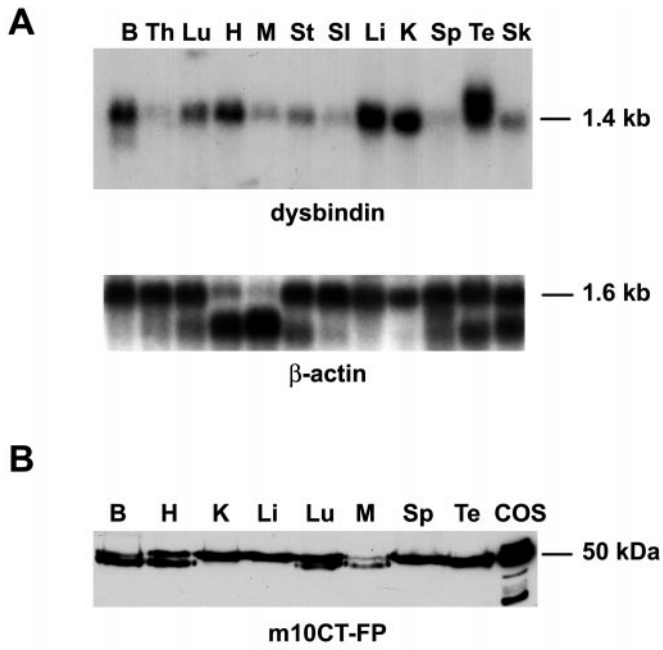

FIG. 3. **Tissue distribution of the dysbindin transcript and protein.** *A*, Northern blot analysis of dysbindin expression. A 1.4-kb transcript is detected abundantly in brain, heart, liver, kidney, and testes (*upper panel*). To demonstrate equal loading, the same blot was stripped and re-hybridized with a β-actin cDNA probe (*lower panel*). *B*, brain; *Th*, thymus; *Lu*, lung; *H*, heart; *M*, skeletal muscle; *St*, stomach; *SI*, small intestine; *Li*, liver; *K*, kidney; *Sp*, spleen; *Te*, testis; *Sk*, skin. *B*, Western blot analysis of dysbindin distribution. The m10CT-FP antibody detects a 50-kDa protein corresponding to dysbindin in all tissues. Dysbindin migrates as a doublet that could be the result of alternative splicing within the dysbindin gene. Note that the lowest levels of dysbindin are detected in skeletal muscle. Dysbindin expressed in COS-7 cells is shown as a control. *B*, brain; *H*, heart; *K*, kidney; *Li*, liver; *Lu*, lung; *M*, muscle; *Sp*, spleen; *Te*, testis; *COS*, COS-7 cells transfected with m10:pCIneo.

essentially negate the possibility that this interaction is mediated by nonspecific coiled-coils. Furthermore, these data suggest that dysbindin binds to the N terminus of dystrobrevin. In control experiments, the effect of β_2-syntrophin and Dp116 expression on the localization of BetaGΔH1+2 was determined. Co-transfection of β_2-syntrophin and BetaGΔH1+2 resulted in the re-distribution of dystrobrevin-immunoreactivity to the cytoplasm and precise co-localization of the two proteins (Fig. 4, *J–L*). As predicted, these data show that β_2-syntrophin does not interact with the coiled-coil region of β-dystrobrevin. By contrast, co-transfection of Dp116 and BetaGΔH1+2 does not result in the re-distribution of β-dystrobrevin to the cytoplasm with both proteins occupying distinct subcellular locations (Fig. 4, *M–O*). These data are consistent with the dystrophin-binding site on dystrobrevin being within the coiled-coil region (20).

Co-transfection of COS-7 cells was also used to confirm that dysbindin and dystrobrevin are directly associated. RIPA cell extracts prepared 24 h after transfection were used for immunoprecipitation with the m10CT-FP or 9E10 antibodies. Co-immunoprecipitated proteins were identified by Western blotting with βCT-FP. Dysbindin co-immunoprecipitated β-dystrobrevin strongly and each of the deletion constructs (Fig. 5). Although the IgG heavy chains obscures BetaGΔH1 and BetaGΔH1+2 in m10CT-FP immunoprecipitates, these proteins are readily visualized when the 9E10 monoclonal antibody is used for immunoprecipitation. α-Dystrobrevin-1 also immunoprecipitates with dysbindin (Fig. 5). The levels of α-dystrobrevin-1 expressed in COS cells are much lower than the levels of the β-dystrobrevins expressed from BetaG (data not shown). Dysbindin failed to co-immunoprecipitate with Dp116 and G-utrophin when co-transfected into COS cells (data not shown). These data suggest that dysbindin is a specific binding partner for the β- and α-dystrobrevin. In control experiments, α-dystrobrevin-1 is immunoprecipitated with m10CT-FP from transfected cells only when m24:pCIneo and myc-m10:pCIneo are co-expressed (Fig. 5*B*).

In Vivo Association of Dysbindin with the DPC—To determine whether dysbindin formed a complex with the dystrobrevins *in vivo*, proteins extracted from rat brain and muscle were immunoprecipitated with the m10CT-FP antibody. Immunoprecipitated proteins were Western-blotted with βCT-FP, the 2166 anti-dystrophin antibody, and the anti-utrophin antibody URD40. m10CT-FP efficiently co-immunoprecipitates α-dystrobrevin-1 and β-dystrobrevin from brain and α-dystrobrevin-1 and -2 from muscle (Fig. 6*A*). Muscle-expressed α-dystrobrevin-2 is difficult to resolve after longer exposure times because it migrates closely to the IgG heavy chain. In control experiments, the dystrobrevins were co-immunoprecipitated directly with a pan-anti-dystrobrevin monoclonal antibody. The same proteins that are precipitated with m10CT-FP are also precipitated with the monoclonal antibody (Fig. 6*B*). In control experiments on brain extracts, the dystrobrevins are only detected when m10CT-FP is used as the precipitating antibody but not when the antibody is omitted (Fig. 6*E*). Thus, m10CT-FP robustly co-immunoprecipitates the dystrobrevins expressed in brain and in muscle, showing that they form a protein complex *in vivo*.

The presence of dystrophin and its isoforms in proteins co-immunoprecipitated with m10CT-FP was determined by immunoblotting with the 2166 antibody (Fig. 6*C*). Dystrophin is detected in proteins co-immunoprecipitated with dysbindin in muscle whereas Dp71 is detected, albeit weakly, in brain immunoprecipitates. Direct comparison of the tissue extracts with the profile of immunoprecipitated proteins shows that only a subset of dystrophin cross-reactive proteins are associated with dysbindin (Fig. 6*C′*). The presence of utrophin among the proteins co-immunoprecipitated with m10CT-FP was determined using the URD40 antibody (Fig. 6*D*). Utrophin co-immunoprecipitates with dysbindin and dystrobrevin in the brain but not in muscle (Fig. 6*D*). This could reflect the low amounts of utrophin relative to dystrophin in muscle, a preferential association of dysbindin with dystrophin rather than utrophin, or compartmentalization of dysbindin in muscle (see below). Western blots of tissue extracts immunoblotted with URD40 shown that the levels of utrophin in RIPA extracts prepared from muscle and brain are similar (Fig. 6*D′*).

Immunolocalization of Dysbindin in Muscle—The m10CT-FP antibody was used to determine the location of dysbindin in normal mouse muscle. Dysbindin immunoreactivity is detected at the sarcolemma of most muscle fibers, in large blood vessels and in endomyosial capillaries (Fig. 7*A*). Dysbindin immunoreactivity was abolished by incubating m10CT-FP with an excess of the immunizing fusion protein confirming the specificity of the antibody (Fig. 7*B*). Interestingly, dysbindin is not enriched at the junctional cytoplasm (Fig. 7, *C* and *D*). Double immunofluorescence with m10CT-FP and Alexa-488-labeled α-bungarotoxin shows reduced dysbindin immunoreactivity in the area of muscle surrounding the NMJ compared with the adjacent sarcolemma (Fig. 7, *C* and *D*).

Double immunofluorescence and confocal microscopy was used to co-localize dysbindin and α-dystrobrevin in muscle. In serial muscle sections, dysbindin clearly co-localizes with α-dystrobrevin at the sarcolemma of most muscle fibers and in large blood vessels (*arrows* in Fig. 7, *E* and *F*). The precise co-localization of both proteins is seen in longitudinal sections of mouse muscle viewed by confocal laser microscopy (Fig. 7, *G*

Downloaded from http://www.jbc.org/ by guest on November 4, 2016

TABLE I
Expression constructs used in this study

The protein encoded by β-dystrobrevin clone BetaG is 555 amino acids and corresponds to amino acids 1–579 of the published sequence (GI 6681235) but lacks the alternatively spliced amino acids (360–390) and (580–608).

Name	Vector	Product	Detecting antibody
m10:pCIneo	pCIneo	Dysbindin	m10CT-FP
myc-m10:pCIneo	pCIneo	Myc-tagged dysbindin	9E10 or m10CT-FP
BetaG	pCIneo	β-Dystrobrevin	β521
BetaGΔH1	pCIneo	β-Dystrobrevin Δ384–450	β521
BetaGΔH2	pCIneo	β-Dystrobrevin Δ451–486	β521
BetaGΔH1+2	pCIneo	β-Dystrobrevin Δ384–486	β521
m32:pCIneo	pCIneo	α-Dystrobrevin-2	βCT-FP
m24:pCIneo	pCIneo	α-Dystrobrevin-1	βCT-FP
pG-utro	pcDNA3	Mouse G-utrophin	URD40
pDp116	pcDNA3	Rat Dp116	2166
β2syn:pCIneo	pCIneo	Mouse β2-syntrophin	SYN1351

and *H*). In this experiment anti-dysbindin immunoreactivity was detected by using an excess of Rhodamine Red-X-labeled $F(ab')_2$ fragments. α-Dystrobrevin was detected in the same sections by using βCT-FP followed by Alexa 488-conjugated anti-rabbit IgG.

Immunolocalization of Dysbindin in Dystrophin-deficient Muscle—To determine the immunolocalization of dysbindin in dystrophin-deficient muscle, sections of *mdx* and normal tibialis anterior muscle were stained with m10CT-FP. m10CT-FP strongly stained the sarcolemma of the *mdx* mouse muscle (Fig. 8, *A* and *B*). By comparing the intensity of anti-dysbindin immunoreactivity at the sarcolemma of normal and *mdx* mice, it can be seen that dysbindin is clearly up-regulated in *mdx* mouse muscle (Fig. 8, *A* and *B*). Dysbindin immunoreactivity is detected strongly at the sarcolemma of all fibers and is coincident with a reduction of intrafiber labeling. To determine whether the increase in dysbindin immunoreactivity at the sarcolemma corresponded to an alteration in the levels of the protein, Western blots of muscle extracts from normal and *mdx* mice were probed with m10CT-FP (Fig. 8*C*). Using densitometric analysis, the levels of dysbindin in total muscle extracts from *mdx* mice are increased approximately 5-fold when compared with the normal muscle. Equivalent loading was demonstrated by comparison of Coomassie Blue-stained gels for total protein content and also with the anti-dystrobrevin antibody βCT-FP. It has been shown previously that, although the levels of α-dystrobrevin-1 in muscle are unaltered in the *mdx* mouse, α-dystrobrevin-2 levels are reduced (26).

Dysbindin Localization in the Brain —We have shown previously that there are multiple dystrophin-like protein complexes in the brain that differ in their dystrobrevin content (18). To determine the location of dysbindin in the brain, m10CT-FP was used to stain mouse brain tissue. In immunoperoxidase-stained sections, the reaction product is confined exclusively to neurons (Fig. 9). There is no significant deposition of reaction product in glial cells. In the cortex, immunoreactive axon profiles are stained in the corpus callosum and are seen ramifying throughout all laminae, taking both vertical and tangential trajectories (Fig. 9*A*). All regions of the hippocampus, the dentate gyrus, CA1-CA3 (Fig. 9*B*), and the fimbria (data not shown) are immunoreactive. There are three distinct types of staining. First, light immunoreactivity is associated with densely packed small punctae in the stratum radiatum and stratum oriens. Second, the axons of the fimbria are weakly stained (Fig. 9*B*). Third, and most prominently, there are intense deposits of reaction product in the afferent mossy fiber terminals in the stratum lucidum. Anti-dysbindin immunoreactivity is also prominent in the cerebellar cortex. As in hippocampus, there is axonal immunoreactivity in the white matter tracts (Fig. 9*C*) together with intense staining of mossy fiber axons and their large terminals in the synaptic glomeruli in the granular layer (Fig. 9, *C–E*). From the density and heterogeneous distribution of the labeled mossy fiber terminals, it is evident that these represent only a small fraction of the total population. There is also lighter punctate immunoreactivity in the molecular layer, consistent with the distribution of synapses between parallel fibers and Purkinje cells (Fig. 9, *C* and *D*). Weak immunoreactivity is associated with axons in the molecular layer of both the dorsal and the ventral cochlear nuclei (Fig. 9, *F* and *G*). In addition, as in the cerebellum, anti-dysbindin immunocytochemistry reveals large, intensely immunoreactive punctae that resemble mossy fiber terminals in the fusiform and deep layers of the dorsal (but not ventral) cochlear. Sparse but robust punctate immunoreactivity is seen throughout the brainstem. For example, in the facial nuclei (Fig. 9*H*) and the spinal trigeminal nuclei (Fig. 9*I*), especially at their lateral edges where they abut the spinal trigeminal tract. In the midbrain there is substantial axonal immunoreactivity for example in the substantia nigra (Fig. 9*J*). Finally, many axon tracts are dysbindin-immunoreactive, including the corpus callosum (Fig. 9*A*), the cerebellar white matter (Fig. 9*D*), and the cranial nerves (*e.g.* Fig. 9*J*). Others stain more weakly, for example the spinal trigeminal tract (Fig. 9, *F* and *I*), the inferior cerebellar peduncles (Fig. 9, *F* and *G*), the fimbria, the facial nerve, and the optic chiasm (data not shown). It is noteworthy that some axon tracts seem to be unreactive, *e.g.* the internal capsule (Fig. 9*J*).

DISCUSSION

The molecular pathology of muscular dystrophy involves an increasing number of proteins and biochemical pathways. It is now accepted that the DPC contains proteins that are involved in intracellular signaling as well as those that fulfil a structural role in maintaining the mechanical stability of the muscle membrane. Furthermore, it seems intuitive to conclude that many components of the DPC contribute directly to the maintenance of muscle integrity. For example, limb-girdle muscular dystrophy patients with mutations in the sarcoglycan genes often have muscular dystrophy without affecting the localization of dystrophin and dystroglycan (39, 40). The α-dystrobrevin-deficient mouse represents an important paradigm for the study of muscular dystrophy. The development of muscular dystrophy in this mouse without perturbation of the DPC strongly suggests that a dystrobrevin-linked signal transduction pathway is involved in the pathogenesis of DMD (8, 9). Thus, proteins associated with α-dystrobrevin in muscle could be involved in similar pathways. In this paper, we describe the characterization of dysbindin, a novel coiled-coil-containing protein that binds to both α- and β-dystrobrevin in muscle and brain.

Dysbindin in Muscle—We have shown that dysbindin binds to α-dystrobrevin and is located at the sarcolemma of normal

Downloaded from http://www.jbc.org/ by guest on November 4, 2016

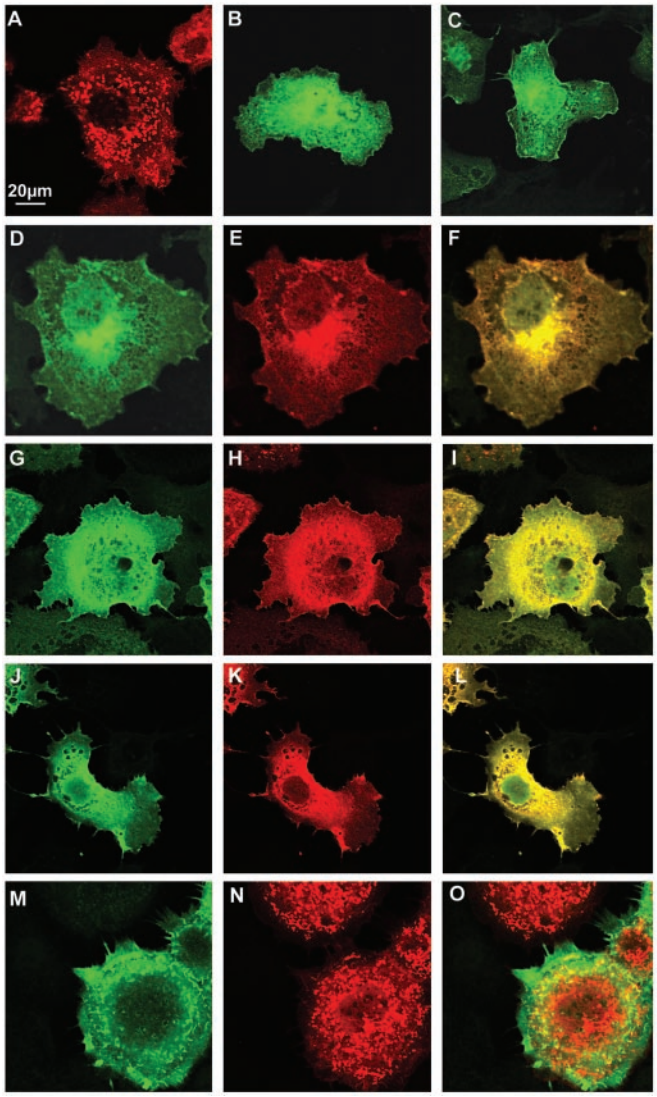

FIG. 4. ***In vitro* co-localization of dysbindin and dystrobrevin in COS-7 cells.** The subcellular distribution of β-dystrobrevin and dysbindin was determined by transfecting COS-7 cells with BetaG (*A*) and myc-m10:pCIneo (*B*) or m10:pCIneo (*C*), respectively. β-Dystrobrevin immunoreactivity appears punctate within the COS cell cytoplasm (*A*), whereas dysbindin is diffusely expressed in the cytoplasm and nucleus (*B* and *C*). The insertion of a Myc epitope tag at the N terminus of the dysbindin protein does not appear to affect its localization (*B*). Co-transfection of myc-m10:pCIneo (*D*) with BetaG (*E*) results in the re-distribution of β-dystrobrevin into the cytoplasm and precise co-localization with dysbindin (*F*). Similar results are obtained when myc-m10:pCIneo (*G*) is co-transfected with BetaGΔH1+2 (*H*). The expression of dysbindin re-localizes β-dystrobrevin protein that lacks the entire coiled-coil domain, resulting in co-localization of the two proteins (*I*). In control experiments, the effect of β_2-syntrophin (*J*) and Dp116 (*M*) on the subcellular localization of BetaGΔH1+2 (*K* and *N*) was determined. Expression of β_2-syntrophin (*J*) causes the re-localization of β-dystrobrevin Δ384–486 (*K*) to the cytoplasm and precise co-localization of the two proteins (*L*). By contrast, co-transfection of pDp116 (*M*) and BetaGΔH1+2 (*N*) has no apparent affect on the localization of β-dystrobrevin Δ384–486 (*N*). These proteins fail to co-localize and are easily resolved (*O*). β-Dystrobrevin was detected with β521 (*A*, *E*, *H*, *K*, and *N*). Dysbindin was detected with 9E10 (*B*, *D*, and *G*) or m10CT-FP (*C*). β_2-Syntrophin was detected with SYN1351 (*J*), and Dp116 was detected with MANDRA1 (*M*). *Panels F*, *I*, *L*, and *O* are the merged images from each experiment. *Scale bar* = 20 μm.

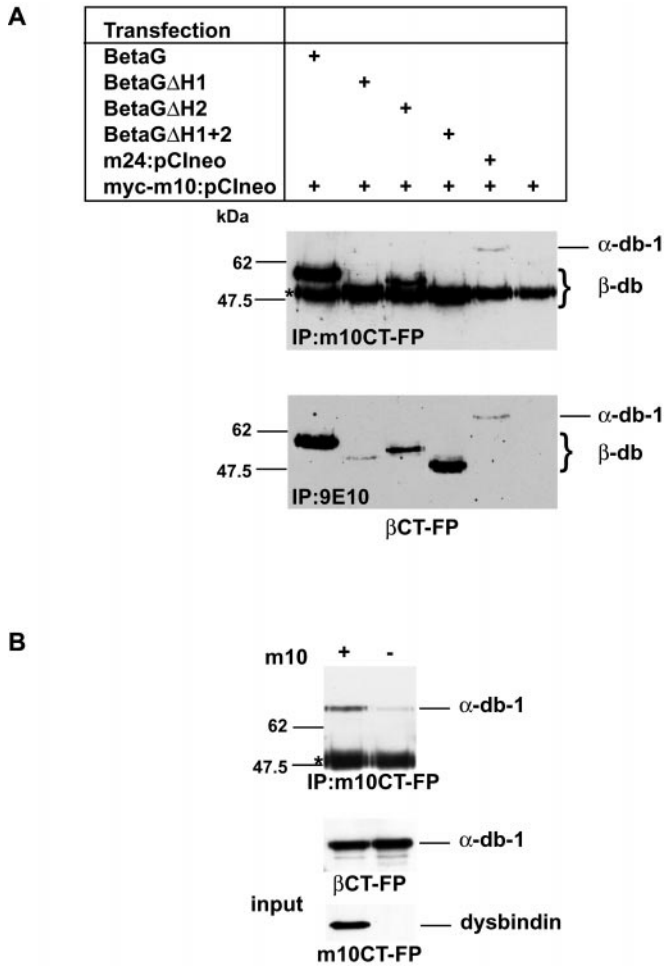

FIG. 5. **In vitro association of dysbindin and dystrobrevin (*db*) in COS-7 cells.** RIPA protein extracts were prepared from cells co-transfected with plasmids as indicated (*A*). Proteins were immunoprecipitated with m10CT-FP and 9E10 and detected with βCT-FP. β-Dystrobrevin is strongly immunoprecipitated by m10CT-FP and 9E10, indicating that dysbindin and β-dystrobrevin form a complex in transfected cells. Similarly, the β-dystrobrevin mutants lacking the coiled coils are immunoprecipitated with appropriate antibodies. The IgG heavy chain (*asterisk*) obscures immunoprecipitated BetaGΔH1 and BetaGΔH1+2; however, these proteins can be clearly resolved when 9E10 is used as the immunoprecipitating antibody (*lower panel*). α-Dystrobrevin-1 is also immunoprecipitated by both antibodies but appears weaker than the β-dystrobrevin constructs because it is not expressed as highly in COS-7 cells. No βCT-FP-immunoreactive proteins are detected when myc-m10:pCIneo is expressed on its own. The sizes of the molecular mass markers in kDa are shown. In control experiments (*B*), α-dystrobrevin-1 is immunoprecipitated robustly from COS-7 cells only when dysbindin is co-expressed (*top panel*). The + indicates co-transfection of m24:pCIneo and myc-m10:pCIneo, whereas the − indicates that only m24:pCIneo was transfected. Western blots of the lysates probed with βCT-FP (*middle panel*) and m10CT-FP (*lower panel*) are shown for comparison. A trace amount of α-dystrobrevin-1 is detected in the − *lane* due to the low levels of endogenous dystrobrevin and dysbindin in COS-7 cells.

muscle. In *mdx* muscle, increased dysbindin immunoreactivity is detected at the sarcolemma coincident with an elevation in the levels of total protein. Although dysbindin is expressed at lower levels in muscle relative to some other tissues, we believe that this interaction is functionally important because dysbindin levels and localization are affected by the absence of dystrophin and dystrobrevin. Most components of the DPC, including α-dystrobrevin, are depleted from the sarcolemma of dystrophin-deficient muscle (16, 41). Several proteins such as utrophin (42), biglycan (43), and filamin-2 (44) are up-regulated in dystrophin-deficient muscle. In these cases the up-regulation appears to be related to a dynamic perturbation in the DPC or to muscle damage. Utrophin up-regulation in dystrophic muscle may be an indicator of muscle damage or regeneration since it occurs in other non-DPC-linked forms of muscular dystrophy (42). Similarly, filamin-2 may also be up-

Downloaded from http://www.jbc.org/ by guest on November 4, 2016

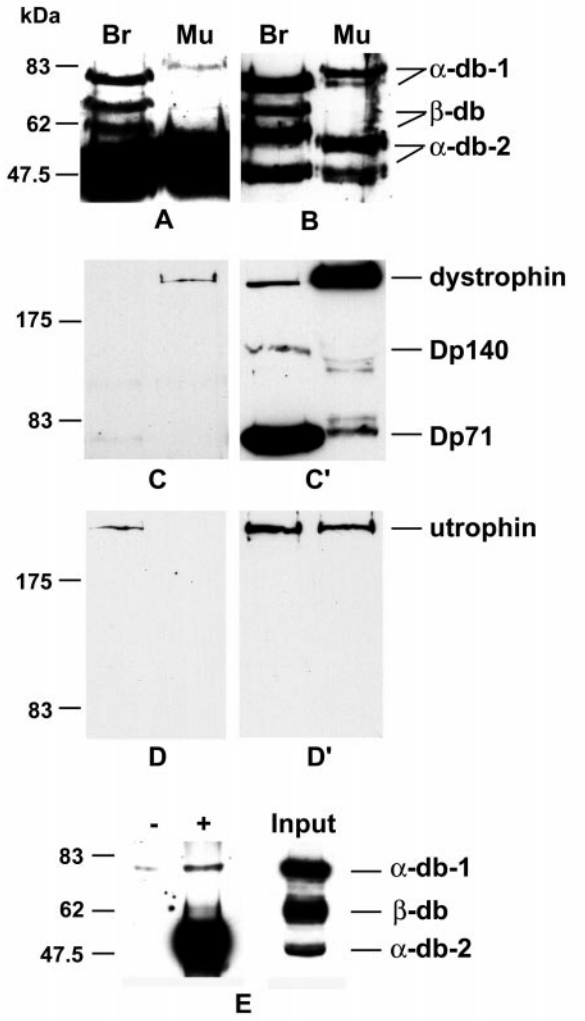

FIG. 6. ***In vivo* association of dysbindin with the DPC.** Proteins extracted from rat brain (*Br*) or muscle (*Mu*) were immunoprecipitated with the anti-dysbindin antibody, m10CT-FP (*A*, *C*, and *D*) or an anti-dystrobrevin monoclonal antibody (*B*). Proteins were detected with βCT-FP (*A* and *B*), the anti-dystrophin antibody 2166 (*C* and *C′*), and the anti-utrophin antibody URD40 (*D* and *D′*). m10CT-FP immunoprecipitates α-dystrobrevin-1 and β-dystrobrevin from brain and α-dystrobrevin-1 and -2 from muscle (*A*). A similar protein profile is seen in whole tissue extracts immunoprecipitated with the anti-dystrobrevin monoclonal antibody (*B*). *Panels C′* and *D′* show dystrophin and utrophin cross-reactive proteins in the appropriate whole tissue extracts. *Panel E* shows that α-dystrobrevin-1 and β-dystrobrevin are immunoprecipitated from brain extracts only in the presence of m10CT-FP (+) and not in its absence (−). The brain extract is shown for comparison. The sizes of the molecular mass markers in kDa are shown.

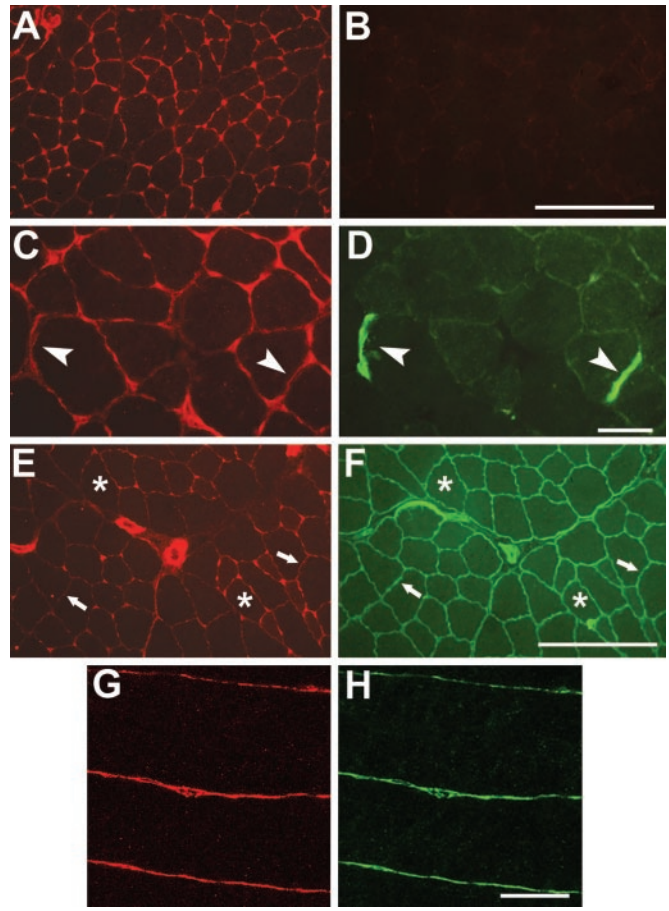

FIG. 7. **Localization of dysbindin in normal muscle. Sections of mouse quadriceps were stained with m10CT-FP.** Dysbindin is seen at the sarcolemma of most fibers but is also found in endomyosial capillaries and other large blood vessels (*A*). Pre-incubation of the m10CT-FP antibody with the immunizing peptide effectively abolishes labeling (*B*). Double immunofluorescence of m10CT-FP detected with a Rhodamine Red-X-conjugated secondary antibody (*C*) and Alexa-488-labeled α-bungarotoxin (*D*) shows that dysbindin does not appear to be concentrated at the junctional cytoplasm. The *arrowheads* identify the position of the NMJs. Co-localization of dysbindin and α-dystrobrevin was established by analysis of serial muscle sections stained with m10CT-FP (*E*) and βCT-FP (*F*). The *asterisks* identify the same muscle fibers in adjacent sections. The *arrows* identify areas where clear co-localization can be seen. To augment the co-localization studies, m10CT-FP (*G*) and βCT-FP (*H*) were used to stain the same muscle sections as described under "Experimental Procedures." Examination of the longitudinal sections demonstrates clear co-localization of both proteins at the muscle sarcolemma. *Scale bars* are 50 μm (*A–F*) and 20 μm (*G* and *H*).

regulated in response to muscle damage since only a small proportion of filamin-2 is associated with the sarcoglycans. Dysbindin up-regulation in the *mdx* mouse differs from the former examples because dysbindin is normally expressed at the sarcolemma albeit at relatively low levels. The up-regulation of dysbindin at the sarcolemma of *mdx* muscle could play a direct role in the pathogenesis of muscular dystrophy.

Recently, the novel intermediate filament protein syncoilin was shown to be associated with α-dystrobrevin-1 in muscle (26). Syncoilin is located at the NMJ in normal muscle and is up-regulated in different mouse models of muscular dystrophy (26). It is noteworthy that dysbindin is not enriched at the junctional sarcolemma but is also up-regulated in the *mdx* mouse. It is therefore possible that dysbindin and syncoilin could play similar roles in different parts of the muscle fiber. However, the function of both proteins remains to be determined.

The interaction between dysbindin and dystrobrevin could provide another mechanism to locate α-dystrobrevin to the muscle sarcolemma. This role is supported by our finding that dysbindin is retained at the sarcolemma in the absence of dystrophin and dystrobrevin (Fig. 8). Thus, the membrane association of dysbindin is independent of the DPC. These findings could also explain the membrane association of dystrobrevin in a dystrophin transgenic mouse lacking exons 71–78 (45). This mouse lacks the described dystrobrevin and syntrophin binding sites in exons 73–75 but still has normal levels of dystrobrevin and syntrophin at the sarcolemma. Whether dysbindin has additional binding partners at the membrane remains to be determined. The identification of such proteins may explain the molecular pathology of dystrobrevin deficiency that appears to be independent of the core DPC (8, 9).

Dysbindin in the CNS—In the adult CNS, dysbindin immu-

Downloaded from http://www.jbc.org/ by guest on November 4, 2016

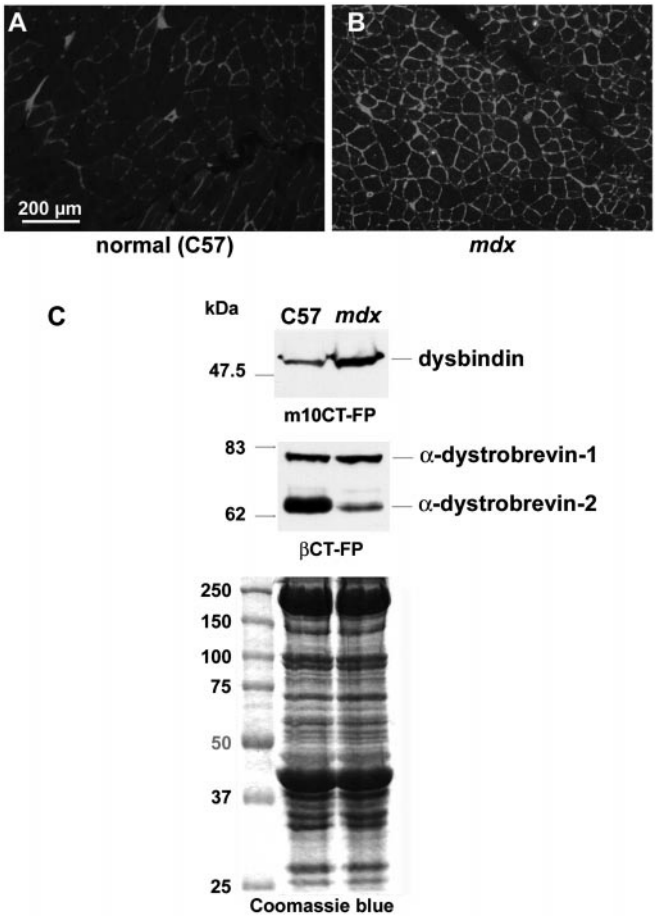

FIG. 8. **Dysbindin in dystrophic muscle.** Sections of normal (*A*) and *mdx* (*B*) tibialis anterior were stained with m10CT-FP. Representative fields were photographed at low power on the correct exposure time for the *mdx* section, allowing for a qualitative estimate of anti-dysbindin immunoreactivity to be attained. To determine whether elevated levels of dysbindin were responsible for the increased immunofluorescence in *mdx* muscle, 50 μg of total protein extracted from normal and *mdx* mouse muscle was Western-blotted and probed with m10CT-FP (*C*). Dysbindin is identified as a 50-kDa protein that is present at higher levels in *mdx* mouse muscle when compared with normal C57 muscle (*top panel*). In control experiments to demonstrate equal loading, a Western blot was incubated with the βCT-FP antibody (*middle panel*). The levels of α-dystrobrevin-1 in the two samples were identical, whereas the levels of α-dystrobrevin-2 are reduced in *mdx* mouse muscle as described (26). Additionally, a Coomassie Blue-stained gel C57 and *mdx* mouse muscle extracts is also shown (*lower panel*). The sizes of the molecular mass markers in kDa are shown.

noreactivity is detected almost exclusively in axons (Fig. 9). This distribution overlaps in part with the localization of β-dystrobrevin in the CNS, notably in axons and in the brain stem (18). The robust co-immunoprecipitation of dysbindin and β-dystrobrevin in brain suggests that β-dystrobrevin and dysbindin probably form a protein complex in axons. There are two distinct types of anti-dysbindin immunoreactivity. The first, in common with β-dystrobrevin, is associated with numerous axon types throughout the brain. The second pattern of dysbindin immunoreactivity is the intense staining that is associated with a small subset of axons, characterized by their large terminals: mossy fibers in the cerebellum, hippocampus, and cochlear nuclei. All of these synapses are very large and glutaminergic. It is unclear whether the intense immunoreactivity is simply a consequence of the large volumes of the terminal structures or if dysbindin has a special role to play at large synaptic terminals. The distribution of cerebellar mossy fibers is also reminiscent of the cholinergic population that terminates predominantly in the vestibulocerebellum (reviewed in

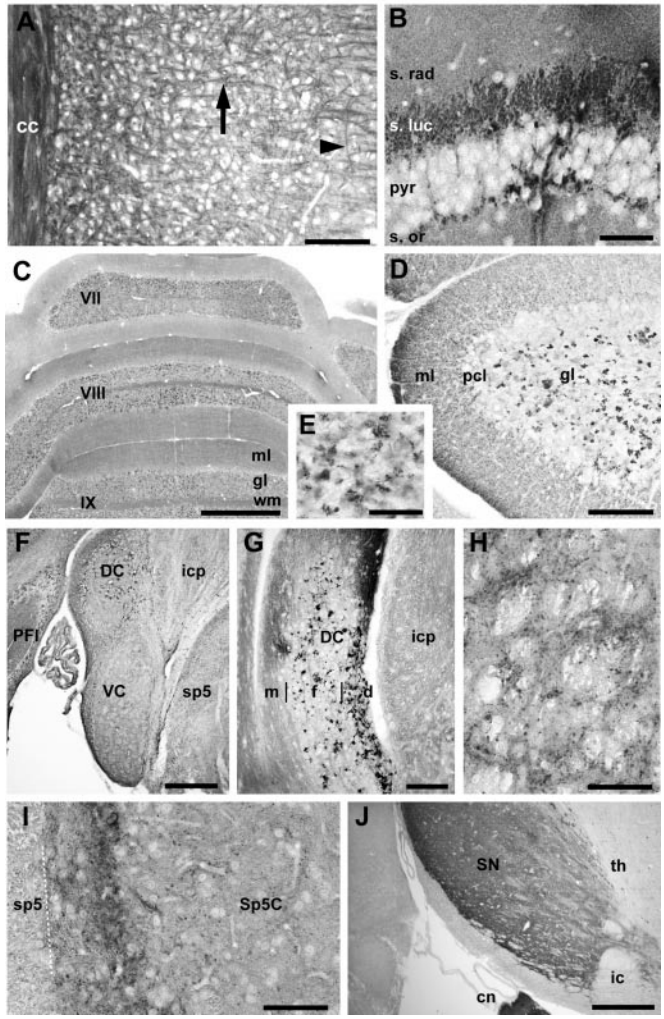

FIG. 9. **Immunoperoxidase anti-dysbindin staining of the adult mouse brain.** In the parietal cortex (*A*), axons are seen exiting from the corpus callosum (*cc*) into all layers of the cortex. Axons run both vertically (*arrow*) and horizontally (*arrowhead*). In the hippocampus (*B*), the reaction product is seen throughout the region (CA3 is shown) in numerous small punctae in the stratum radiatum (*s. rad*) and stratum oriens (*s. or*), and intensive labeling is associated with the mossy fiber terminals in the stratum lucidum (*s. luc*). The pyramidal cells (*pyr*) appear unreactive. *C–E*, cerebellum. The reaction product is deposited in the white matter tracts (*wm*) and in the granular layer (*gl*) throughout the cerebellar cortex, but most intensely in the posterior lobe vermis (illustrated in *C*) and the flocculus and paraflocculus. Lobule X is seen in higher magnification in sagittal section (*D*). Light, punctate staining is seen in the molecular layer (*ml*). Purkinje cell layer (*pcl*) immunoreactivity is very weak or absent. In the *inset* in *E*, the stained mossy fiber terminals in the granular layer (the synaptic glomeruli) are shown at higher magnification. *F* and *G*, cochlear nuclei. Prominent mossy fiber immunoreactivity is detected in the fusiform (*f*) and deep (*d*) layers of the dorsal cochlear (*DC*) but not in the ventral cochlear (*VC*) nuclei. Additional fine axonal staining is seen throughout the molecular layer (*m*). In neighboring structures, axons are weakly stained in the spinal trigeminal tract (*sp5*) and the inferior cerebellar peduncle (*icp*), and mossy fiber labeling is prominent laterally in the cerebellar paraflocculus (*PFl*). *H*, facial nucleus. Intensely stained punctae are scattered throughout the facial nucleus. *I*, spinal trigeminal. Weak immunoreactivity is associated with the axons of the spinal trigeminal tract (*sp5*) and with numerous small, strongly-reacting punctae in the caudal spinal trigeminal nucleus (*Sp5C*), especially at its lateral margin where it abuts the spinal trigeminal tract (*dashed line*). *J*, substantia nigra. Axons are stained throughout the substantia nigra (*SN*). By contrast, there is little or no immunoreactivity in the axons of the internal capsule (*ic*) or in the thalamus (*th*). There is also strong immunoreactivity in the cranial nerves (*cn*). *Sections D* and *F* are sagittal; the others are transverse. *Scale bars*, 100 μm (*A*, *D*, and *G*), 50 μm (*B*, *E*, *H*, and *I*), 250 μm (*F* and *J*), and 500 μm (*C*).

Downloaded from http://www.jbc.org/ by guest on November 4, 2016

Ref. 46), indicating that there is no simple correlation with dysbindin immunoreactivity and neurotransmitter phenotype.

The concentration of dysbindin in axon terminals suggests a presynaptic localization. Whereas β-dystrobrevin and dystrophin are thought to be postsynaptic proteins (18, 47), in the retina dystrophin immunoreactivity is exclusively presynaptic (48, 49). It is therefore possible that DPC-like complexes exist at the presynaptic membrane as well as the postsynaptic membrane in some populations of neurons.

The association of dysbindin with α-dystrobrevin-1 is less clear. α-Dystrobrevin-1 is expressed in glia, notably perivascular astrocytes, and in vascular endothelial cells (18, 50). Although utrophin was originally thought to be enriched in astrocytic foot processes (51), recent high resolution confocal microscopy has shown that utrophin is found in the endothelium of blood vessels and in some neurons (52). Dysbindin is expressed in blood vessels in muscle (Fig. 7*A*) and in other tissues such as kidney and liver (data not shown). Thus, a complex of dysbindin, α-dystrobrevin-1, and utrophin could exist in the epithelium of some cranial blood vessels. Consistent with this idea we find a complex of dysbindin, dystrobrevin, and utrophin in the brain (Fig. 6, *A* and *D*).

In summary, we have shown that the dystrobrevins bind to a novel coiled-coil containing protein, dysbindin, which is widely expressed. Dysbindin is up-regulated at the sarcolemma of dystrophin-deficient muscle, suggesting that is involved in the pathogenesis of muscular dystrophy. The identification of this interaction should help to define the role of the dystrobrevins in muscular dystrophy.

Acknowledgments—We are grateful to Profs. Stanley Froehner and Glenn Morris for supplying antibodies. We also thank Prof. Kay Davies for support and encouragement, Dr. Chris Ponting for helpful discussions, Estrella Gonzales for excellent technical support, and Kara Hunter for help with confocal microscopy.

REFERENCES

1. Blake, D. J., and Kroger, S. (2000) *Trends Neurosci.* **23,** 92–99
2. Ozawa, E., Yoshida, M., Suzuki, A., Mizuno, Y., Hagiwara, Y., and Noguchi, S. (1995) *Hum. Mol. Genet.* **4,** 1711–1716
3. Straub, V., and Campbell, K. P. (1997) *Curr. Opin. Neurol.* **10,** 168–175
4. Michalak, M., and Opas, M. (1997) *Curr. Opin. Neurol.* **10,** 436–442
5. Menke, A., and Jockusch, H. (1991) *Nature* **349,** 69–71
6. Petrof, B. J., Shrager, J. B., Stedman, H. H., Kelly, A. M., and Sweeney, H. L. (1993) *Proc. Natl. Acad. Sci. U. S. A.* **90,** 3710–3714
7. Pasternak, C., Wong, S., and Elson, E. L. (1995) *J. Cell Biol.* **128,** 355–361
8. Bredt, D. S. (1999) *Nat. Cell Biol.* **1,** E89–E91
9. Grady, R. M., Grange, R. W., Lau, K. S., Maimone, M. M., Nichol, M. C., Stull, J. T., and Sanes, J. R. (1999) *Nat. Cell Biol.* **1,** 215–220
10. Kameya, S., Miyagoe, Y., Nonaka, I., Ikemoto, T., Endo, M., Hanaoka, K., Nabeshima, Y., and Takeda, S. (1999) *J. Biol. Chem.* **274,** 2193–2200
11. Wagner, K. R., Cohen, J. B., and Huganir, R. L. (1993) *Neuron* **10,** 511–522
12. Blake, D. J., Nawrotzki, R., Peters, M. F., Froehner, S. C., and Davies, K. E. (1996) *J. Biol. Chem.* **271,** 7802–7810
13. Sadoulet-Puccio, H. M., Khurana, T. S., Cohen, J. B., and Kunkel, L. M. (1996) *Hum. Mol. Genet* **5,** 489–496
14. Peters, M. F., O'Brien, K. F., Sadoulet-Puccio, H. M., Kunkel, L. M., Adams, M. E., and Froehner, S. C. (1997) *J. Biol. Chem.* **272,** 31561–31569
15. Blake, D. J., Nawrotzki, R., Loh, N. Y., Gorecki, D. C., and Davies, K. E. (1998) *Proc. Natl. Acad. Sci. U. S. A.* **95,** 241–246
16. Nawrotzki, R., Loh, N. Y., Ruegg, M. A., Davies, K. E., and Blake, D. J. (1998) *J. Cell Sci.* **111,** 2595–2605
17. Peters, M. F., Sadoulet-Puccio, H. M., Grady, M. R., Kramarcy, N. R., Kunkel, L. M., Sanes, J. R., Sealock, R., and Froehner, S. C. (1998) *J. Cell Biol.* **142,** 1269–1278
18. Blake, D. J., Hawkes, R., Benson, M. A., and Beesley, P. W. (1999) *J. Cell Biol.* **147,** 645–658
19. Blake, D. J., Tinsley, J. M., Davies, K. E., Knight, A. E., Winder, S. J., and Kendrick-Jones, J. (1995) *Trends Biochem. Sci.* **20,** 133–135
20. Sadoulet-Puccio, H. M., Rajala, M., and Kunkel, L. M. (1997) *Proc. Natl. Acad. Sci. U. S. A.* **94,** 12413–12418
21. Newey, S. E., Benson, M. A., Ponting, C. P., Davies, K. E., and Blake, D. J. (2000) *Curr. Biol.* **10,** 1295–1298
22. Brenman, J. E., Chao, D. S., Gee, S. H., McGee, A. W., Craven, S. E., Santillano, D. R., Wu, Z., Huang, F., Xia, H., Peters, M. F., Froehner, S. C., and Bredt, D. S. (1996) *Cell* **84,** 757–767
23. Lumeng, C., Phelps, S., Crawford, G. E., Walden, P. D., Barald, K., and Chamberlain, J. S. (1999) *Nat. Neurosci.* **2,** 611–617
24. Hasegawa, M., Cuenda, A., Spillantini, M. G., Thomas, G. M., Buee-Scherrer, V., Cohen, P., and Goedert, M. (1999) *J. Biol. Chem.* **274,** 12626–12631
25. Gee, S. H., Madhavan, R., Levinson, S. R., Caldwell, J. H., Sealock, R., and Froehner, S. C. (1998) *J. Neurosci.* **18,** 128–137
26. Newey, S. E., Howman, E. V., Ponting, C. P., Benson, M. A., Nawrotzki, R., Loh, N. Y., Davies, K. E., and Blake, D. J. (2001) *J. Biol. Chem.* **276,** 6645–6655
27. Gietz, R. D., and Schiestl, R. H. (1995) *Methods Mol. Cell. Biol.* **5,** 255–269
28. Altschul, S. F., Madden, T. L., Schaffer, A. A., Zhang, J., Zhang, Z., Miller, W., and Lipman, D. J. (1997) *Nucleic Acids Res.* **25,** 3389–4302
29. Lupas, A., Van Dyke, M., and Stock, J. (1991) *Science* **252,** 1162–1164
30. Blake, D. J., Love, D. R., Tinsley, J., Morris, G. E., Turley, H., Gatter, K., Dickson, G., Edwards, Y. H., and Davies, K. E. (1992) *Hum. Mol. Genet.* **1,** 103–109
31. Froehner, S. C., Murnane, A. A., Tobler, M., Peng, H. B., and Sealock, R. (1987) *J. Cell Biol.* **104,** 1633–1646
32. Nguyen, T. M., Ginjaar, I. B., van Ommen, G. J., and Morris, G. E. (1992) *Biochem. J.* **288,** 663–668
33. Blake, D. J., Schofield, J. N., Zuellig, R. A., Gorecki, D. C., Phelps, S. R., Barnard, E. A., Edwards, Y. H., and Davies, K. E. (1995) *Proc. Natl. Acad. Sci. U. S. A.* **92,** 3697–3701
34. Schofield, J. N., Blake, D. J., Simmons, C., Morris, G. E., Tinsley, J. M., Davies, K. E., and Edwards, Y. H. (1994) *Hum. Mol. Genet.* **3,** 1309–1316
35. Adams, M. E., Butler, M. H., Dwyer, T. M., Peters, M. F., Murnane, A. A., and Froehner, S. C. (1993) *Neuron* **11,** 531–540
36. Armstrong, C. L., Krueger-Naug, A. M., Currie, R. W., and Hawkes, R. (2000) *J. Comp. Neurol.* **416,** 383–397
37. Ahn, A. H., and Kunkel, L. M. (1995) *J. Cell Biol.* **128,** 363–371
38. Dwyer, T. M., and Froehner, S. C. (1995) *FEBS Lett.* **375,** 91–94
39. Vainzof, M., Passos-Bueno, M. R., Canovas, M., Moreira, E. S., Pavanello, R. C., Marie, S. K., Anderson, L. V., Bonnemann, C. G., McNally, E. M., Nigro, V., Kunkel, L. M., and Zatz, M. (1996) *Hum. Mol. Genet.* **5,** 1963–1969
40. Crosbie, R. H., Lim, L. E., Moore, S. A., Hirano, M., Hays, A. P., Maybaum, S. W., Collin, H., Dovico, S. A., Stolle, C. A., Fardeau, M., Tome, F. M., and Campbell, K. P. (2000) *Hum. Mol. Genet.* **9,** 2019–2027
41. Ervasti, J. M., Ohlendieck, K., Kahl, S. D., Gaver, M. G., and Campbell, K. P. (1990) *Nature* **345,** 315–319
42. Helliwell, T. R., Man, N. T., Morris, G. E., and Davies, K. E. (1992) *Neuromuscul. Disord.* **2,** 177–184
43. Bowe, M. A., Mendis, D. B., and Fallon, J. R. (2000) *J. Cell Biol.* **148,** 801–810
44. Thompson, T. G., Chan, Y. M., Hack, A. A., Brosius, M., Rajala, M., Lidov, H. G., McNally, E. M., Watkins, S., and Kunkel, L. M. (2000) *J. Cell Biol.* **148,** 115–126
45. Crawford, G. E., Faulkner, J. A., Crosbie, R. H., Campbell, K. P., Froehner, S. C., and Chamberlain, J. S. (2000) *J. Cell Biol.* **150,** 1399–1410
46. Jaarsma, D., Ruigrok, T. J., Caffe, R., Cozzari, C., Levey, A. I., Mugnaini, E., and Voogd, J. (1997) *Prog. Brain Res.* **114,** 67–96
47. Lidov, H. G., Byers, T. J., Watkins, S. C., and Kunkel, L. M. (1990) *Nature* **348,** 725–728
48. Ueda, H., Kobayashi, T., Mitsui, K., Tsurugi, K., Tsukahara, S., and Ohno, S. (1995) *Invest. Ophthalmol. Visual Sci.* **36,** 2318–2322
49. Blank, M., Koulen, P., Blake, D. J., and Kroger, S. (1999) *Eur. J. Neurosci.* **11,** 2121–2133
50. Ueda, H., Baba, T., Terada, N., Kato, Y., Fujii, Y., Takayama, I., Mei, X., and Ohno, S. (2000) *Neurosci. Lett.* **283,** 121–124
51. Khurana, T. S., Watkins, S. C., and Kunkel, L. M. (1992) *J. Cell Biol.* **119,** 357–366
52. Knuesel, I., Bornhauser, B. C., Zuellig, R. A., Heller, F., Schaub, M. C., and Fritschy, J. M. (2000) *J. Comp. Neurol.* **422,** 594–611

Downloaded from http://www.jbc.org/ by guest on November 4, 2016

Dysbindin, a Novel Coiled-coil-containing Protein That Interacts with the Dystrobrevins in Muscle and Brain

Matthew A. Benson, Sarah E. Newey, Enca Martin-Rendon, Richard Hawkes and Derek J. Blake

J. Biol. Chem. 2001, 276:24232-24241.
doi: 10.1074/jbc.M010418200 originally published online April 20, 2001

Access the most updated version of this article at doi: 10.1074/jbc.M010418200

Alerts:
- When this article is cited
- When a correction for this article is posted

Click here to choose from all of JBC's e-mail alerts

This article cites 52 references, 30 of which can be accessed free at
http://www.jbc.org/content/276/26/24232.full.html#ref-list-1

Downloaded from http://www.jbc.org/ by guest on November 4, 2016